NEW CHARACTERIZATION OF SAR MODE ALTIMETRY DATA OVER INLAND WATERS

Pierre Fabry[(1)] and Nicolas Bercher[(1)]

[(1)]ALONG-TRACK S.A.S., 43B rue de Bertheaume, 29217, Plougonvelin, France

pfabry@along-track.com

ABSTRACT

Radar altimetry over the inland water domain is a difficult topic that still requires a lot of human expertise as well as manual editing and verifications. This is mainly due to the fact that inland water scenes are highly variable, both in space and time, which leads to a much broader range of radar signatures than in oceanography. The remark is particularly true for LRM altimetry and remains valid in many cases in SAR mode (SARM). In preparation for the operational Sentinel-3 mission and to better benefit from the improved SARM along-track resolution it is required to:

1. better characterize the SARM Individual Echoes, Multi-Look Stacks, 20Hz waveforms as well as the Range Integrated Power (RIP) over the inland water domain,
2. step toward processing schemes that account for the actual content of the illuminated scene.

In this work, we introduce an automated technique to assess the water fraction within the Beam-limited Doppler footprint through its intersection area of with a water mask. This framework opens up new ways toward the automated characterization and processing of altimetry, in the future, thanks to regularly updated water masks.

1. CONTEXT

The main reason why Space Hydrology is still not operational at global scale is the variety of inland water scenes and scenarios which cannot properly be taken into account via a single and fixed processing chain. The complexity coming from the spatial diversity is emphasized by the strong temporal variability related to seasonal trends, extreme events and human action. Rivers and lakes' bathymetry and contours do change over time. Sand banks and islands appear, disappear or change from shape and location. In addition, the radar backscatter properties of water depend on wind conditions, surface current and trophic phenomenons. Not to forget the specific cases of mountain lakes and the vicinity of cities or other strong radar reflectors. Several of these aspects may be mixed together at small spatial scale (few km).

Figure 1 illustrates the complexity of LRM radar altimeter waveforms (Jason-2) on a “standard” case in the Amazon (rio Madeira) involving water and forest surfaces. Figure 2 confirms that CryoSat-2 SAR mode also exhibit portions of hyperboles due to dominant across-track off-nadir water areas (Amazon).

As a matter of fact it has already been shown that SARM radar echoes are sensitive to strong off nadir reflectors. This is depicted by the “loss” of the ground tracks pattern in Figure 3 that plots CryoSat-2 SARin products over the Amazon [Bercher et al., 2014a].

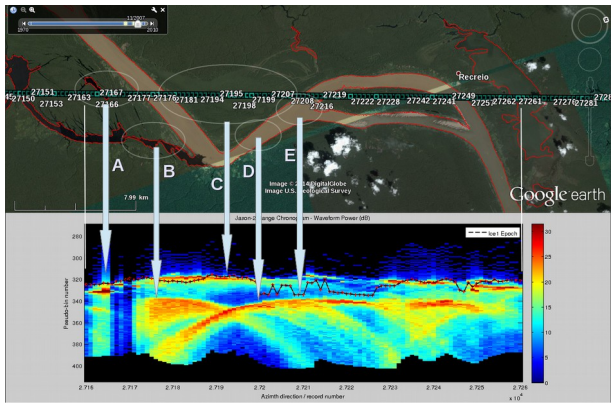

Figure 1. Jason-2 waveforms Range-Chronogram (S-GDR products) over the Madeira river (Brazil). The ICE1 retracker outputs are superimposed (red crosses linked by a black line). ICE1 provides the range in between two water bodies (B and C) while the Range-Chronogram shows the hyperbolic signatures of these two water bodies. The situation is worse in the vicinity of water bodies C, D, E.

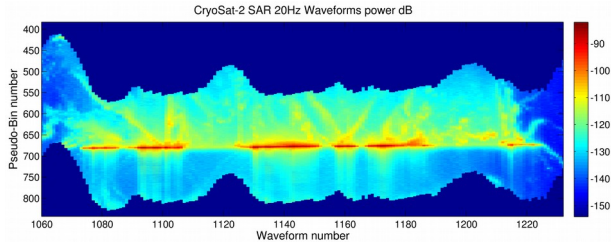

Figure 2. CryoSat-2 SAR 20Hz waveforms Range-Chronogram over multiple water areas in the Amazon. Data kindly provided by Salvatore Dinardo, Nov. 2012 (ESA).

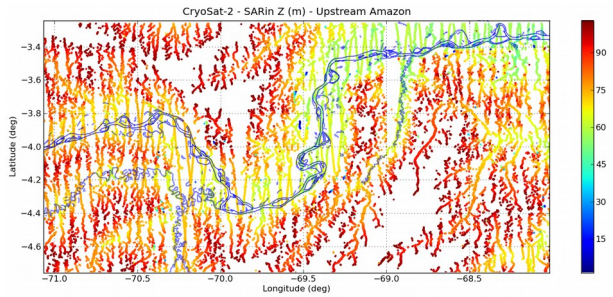

Figure 3. CryoSat-2 ESA/L2 SARin products upstream Amazon. The “loss” of the ground tracks pattern confirms that the altimeter is sensitive enough to very off-nadir water targets.

The inland water scenarios is not only very diverse but also subject to space and time variability. These properties combine with the off-nadir sensitivity of the instrument and result in the loss of accuracy and precision in alti-hydrology measurements. This occurs through land contamination at nadir and multiple off-nadir water contributions. Even repeat orbit altimeters which permit the use of Fixed Virtual Stations (FVS) also described in the literature as Fixed Satellite Gauging Stations (FSGS) are subject to such disturbances.

In this context, how can we use CryoSat-2 data to characterize Sentinel-3 waveforms over inland waters ? And also, how can we derive water heights with a consistent accuracy and precision over time in both SARM and LRM ?

To our point of view FVS should not be used. FVS are manually defined as the intersection area of satellite track and a static pre-defined riverbed, which 1st is too much work to cover the whole globe, 2nd is too sensitive to orbit change or drift (e.g., SARAL mission) and local morphological changes. The delimitation of Satellite Gauging Stations should be adaptive to the actual inland water “ground truth”. For this reason we set up a new framework that enables the automated exploitation of water masks.

2. A NEW AND FLEXIBLE FRAMEWORK FOR ALTI-HYDROLOGY

In the previous section we established that the proper handling of radar altimeter data goes through the best possible use of a priori information on the water content within the instrument footprint. In this section, we introduce a new framework to permit the automated characterisation and editing / masking of Level-1 SARM altimetry data from the a priori knowledge of the water fraction within the instrument footprint.

This new framework is run here with the existing SRTM Water Body Delineation masks (SWBD). It is also a trampoline to the synergistic inter-operation with water masks derived from radar imaging missions such as Sentinel-1 (and ENVISAT for example in the past). Even-though C band radar imagers are lower resolution than optical imagers, their main advantage is to ensure the regular update of water masks thanks to their all-weather and night and day imaging capabilities.
ALONG-TRACK S.A.S. initiated in-house works that will soon exploit Sentinel-1 data in order to produce up-to-date water masks [Fabry et al. 2015a]. They will be used in synergy with CryoSat-2 and Sentinel-3 data to :

- improve the characterization of L1B data products and possibly backward analyse L1A and L1B-S data products,
- improve water height measurements selection at the output of the existing retrackers output even though they are not designed for the inland water domain.

2.1. Principles

Beam-Doppler limited footprint are computed, at each record, from the longitude, latitude, tracker range, satellite altitude and velocity found in the CryoSat-2 L1B product files and the system parameters (3dB antenna beam-width, burst PRF). As depicted in Figure 4 (and zoomed in Figure 5), the Beam-Doppler limited footprints are superimposed with the water masks in the local Earth-tangential plane (ENU: East North-Up). This makes it possible to compute, for each footprint, the footprint area (FA) as well as the water area (WA) at the intersection with the water masks. We then define the **water fraction** as WFR = WA / FA.

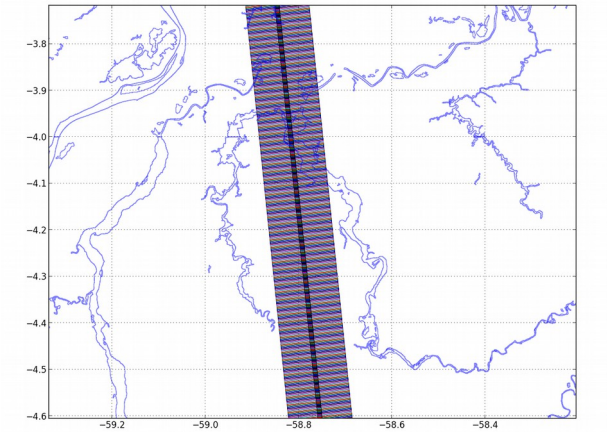

Figure 4. SRTM/SWBD water masks (tiles: w059s04s, w059s05s, w060s04s, w060s05s) superimposed with the series of CryoSat-2 Beam-Doppler limited footprints (20Hz records) generated over small tributaries of the Madeira and Amazon rivers. Baseline B, SAR L1B data on 2014-04-16-T090624.

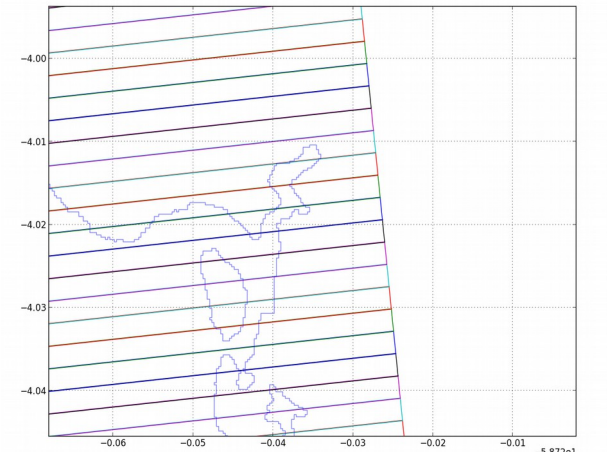

Figure 5. Zoom on the upper central part of Figure 4.

2.2. Details of the Footprints generation

The along-track or Doppler limited footprint size, illustrated in Figure 6, is related to the satellite $_{velocity\ Vsat}$, central wavelength λ, its range to ground *h* and the burst *PRF* :

$$\Delta x = h.\frac{\lambda}{2V_{sat}}.\frac{PRF}{64}$$

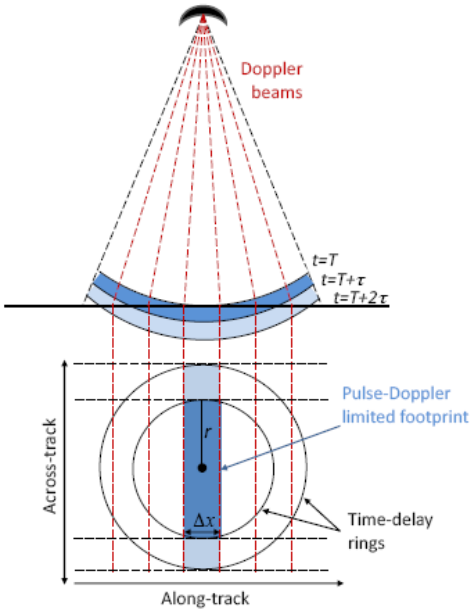

Figure 6. Illustration of the along-track or Doppler limited footprint size, taken from the [CryoSat-2 Handbook, 2013].

A reasonable approximation of the across-track beam size *D* is:

$$D = h.\tan(\theta_B + \frac{\upsilon}{2}) - h.\tan(\theta_B - \frac{\upsilon}{2})$$

where,

- θ_B is the 3dB across-track antenna aperture (1.2 deg),
- υ is the boresight angle w.r.t. nadir (0 deg in this study but it can be computed from the attitude angles and several rotations in the satellite centred reference frame).

Both Δ*x* and *D* are computed at each record's location with the updated parameters and the pixel numbers N and NW as well as the water fraction WFR are derived from the intersection with the water mask.

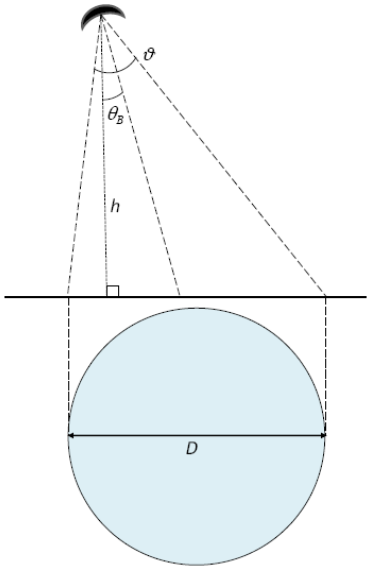

Figure 7. Illustration of the beam limited footprint size, taken from the [CryoSat-2 Handbook, 2013].

2.3. Use of the framework for SARM data characterization

We now use the new framework to check whether the Range Integrated Power Distributions[1] (RIP) have remarkable properties as a function of the WFR, or not. While reading the acquisition parameters for each record and building the Beam-Doppler limited footprints we also access the beam behaviour parameters contained in the L1B products. The following parameters are derived from the fit of the RIP with a Gaussian PDF :

– Stack Scaled : the stack amplitude is scaled so that the power waveform echo sample values all to fit between 0 and 65535 (CryoSat-2 Product Handbook). These samples can then be converted to a power in Watts from: Power [Watts] = scaled value*scalefactor*10^{-9}*$2^{\text{scale power}}$

– Mean Centre of the Gaussian PDF fitting the RIP,

– Stack Standard Deviation of the Gaussian PDF fitting the RIP,

– Stack Skewness : asymmetry of the RIP,

– Stack Kurtosis : peakiness of the RIP.

3. EXPERIMENTAL SET UP

The experiment is performed over 86 CryoSat-2 Baseline B, L1B files in SARM. The study period extends from 2014-01-03 to 2014-02-12. We consider a wide area around the confluence of rio Xingu with the Amazon. The water masks covering this area are in the following SWBD tiles: 'w052s02s', 'w052s03s', 'w053s02s' and 'w053s03s'. The records are selected for the experiment whenever the re-synthesised Beam-Doppler footprint entirely falls inside a tile of interest.

1 RIP. is a 1D signal resulting from the range-wise summation of the 2D Multi-Look Stack (1 stack per record), while the sum in the along-track direction provides the 20Hz SAR waveform.

4. RESULTS

The histogram in Figure 8 illustrates the natural land cover distribution of non-water (WFR=0) and water (WFR>0) surfaces where low WFR classes are over-populated compared to the others. This distribution is also biased by (1) limitations inherent to the design of the SWBD water masks from which water surfaces under a given threshold (about 100m) are discarded [SRTM, 2003] and (2) possible surface classification errors in SWBD tiles. Also, in order to compare classes with similar populations we should process more files and randomly reject some members in the over-populated classes.

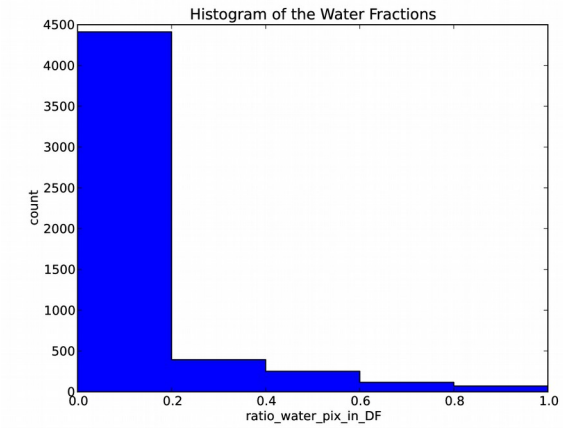

Figure 8. Histogram of the Water Fraction found in the Beam-Doppler footprints of the processed CryoSat-2, L1B, SARM data.

Despite the unbalanced populations, the backscattered energy in classes with a high WFR seems to be better **confined** and consistent than those with low WFR. This trend appears in Figure 9 where the scaled amplitude of the RIP is plotted versus the WFR.

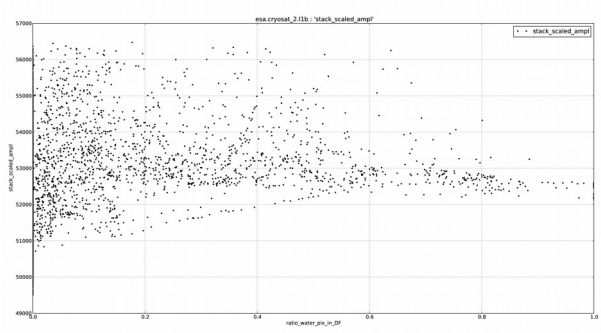

Figure 9. Scaled amplitude of the RIP versus the Water Fraction in the Beam-Doppler footprints.

Indeed, in the low WFR cases the water bodies are diversely spread over the footprint, going from “most of the water area is at nadir” to “most of the water area is at far end” of the footprint. The combination of the antenna diagram and the water surface backscattering diagram are then responsible of a higher diversity in the backscattered power. This is valid in both directions of the stack (along-track for the RIP and across-track for the waveforms) which in turn impacts the scaling factor.

The RIP Standard Deviation indicates how the energy is backscattered from the footprint area into the many azimuth look angles (Doppler Beams). Figure 10 seems to indicate that footprints with a very small water content statistically have a small RIP Standard Deviation (beam to beam response is peaky). This would be in agreement with the fact that small bright targets are more specular in general (less sensitive to wind stress) and the small river legs of the downstream Amazon basin do not experience high surface currents ; they are smooth surfaces in most cases. Nevertheless the low WFR class is quite heterogeneous. On the opposite footprints with a WFR above 80% have a larger RIP Standard Deviation. They exhibit strong backscatter properties in all directions (in all looks) due to a higher roughness (higher wind fetch and surface current).

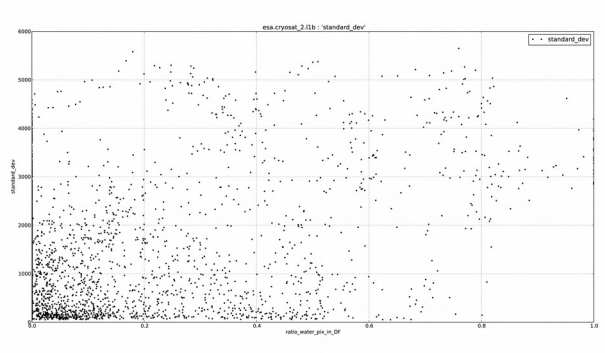

Figure 10. Standard Deviation of the Gaussian PDF fitting the RIP versus the Water Fraction in the Beam-Doppler footprints.

The Stack Centres in Figure 11 seem to vary more for the very low WFR (<15%) than for other classes, which confirms the diversity of this class and the sensitivity to bright targets or along-track slopes in the absence of bright targets (the Point Of Closest Approach is not located at nadir anymore).

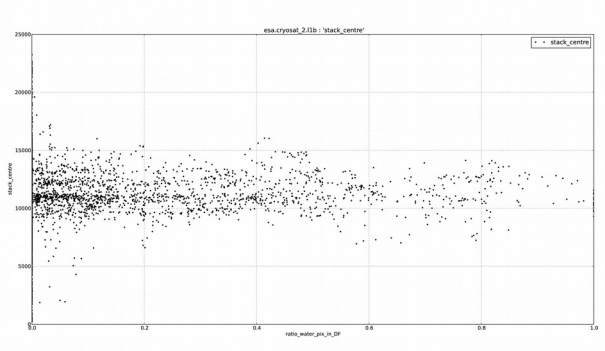

Figure 11. Stack Centre versus the Water Fraction in the Beam-Doppler footprints.

In practice the actual power of the many looks (and therefore the shape of the RIP) is impacted by several contributions:

- the water fraction (WFR),
- the distribution of water bodies across the Doppler Footprint,
- the along-track evolution of the WFR combined to the antenna side lobes. The looks for which a side lobe is directed to a water area will have a ghost contribution to the RIP, thus modifying the shape of the RIP and the Gaussian fit,
- The contribution of small water surfaces not accounted for in SWBD water masks.

In the following part we try to identify potential relationships between the RIP parameters according to the WFR. Figure 12 and 13 seems to indicate that high RIP Standard Deviation values are often associated to low Kurtosis values and these correspond to high WFR cases (purple dots). In other words a fat RIP (wide angular response) is observed when most of the footprint is over water. In the opposite, peaky RIPs correspond to small water content as well as a wide diversity of other cases.

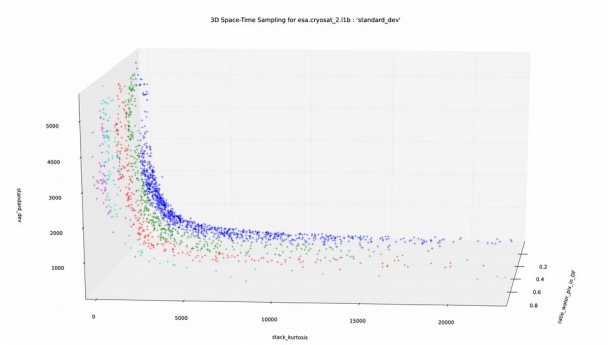

Figure 12. Standard Deviation of the Gaussian PDF fitting the RIP versus the Kurtosis of the RIP and Water Fraction in the Beam-Doppler footprints. WFR are split into 5 coloured classes 20% wide.

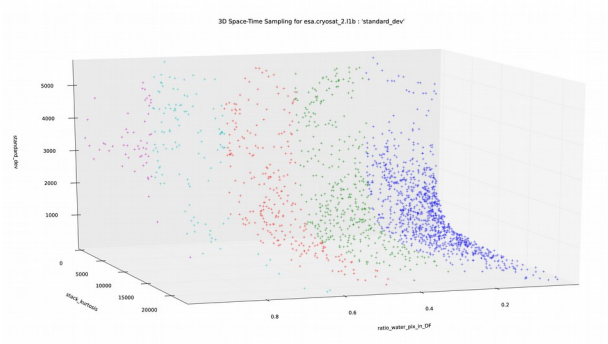

Figure 13. same as figure 12 from another view point.

In addition, figures 14 and 15 show that the high WFR cases correspond to a high symmetry of the RIP (low Skewness) while low WFR cases correspond to a higher asymmetry. This may be due to the fact that in these scenes the non water contribution becomes important in the determination of the along-track angular response. The scene content and morphology as well as the acquisition geometry with respect to the scene content may have a stronger impact onto the beam to beam evolution of the backscattered power.

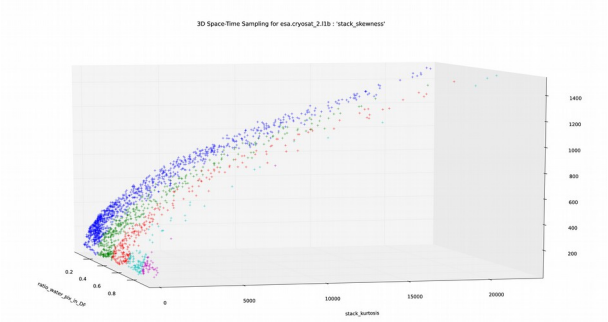

Figure 14. Skewness of the RIP versus the Kurtosis of the RIP and Fraction of Water Pixels in the Beam-Doppler footprints. WFR are split into 5 coloured classes 20% wide.

Figure 15. same as figure 14 from another view point.

5. CONCLUSIONS

Our main objective in this study was to establish a new framework and to have a quick check whether the Range Integrated Power parameters have remarkable features versus the Water Fraction. There is no clear readout of the results since many issues are still entangled together :

1. We probably did not process enough data and, as shown in the histogram, high water fraction footprints are poorly represented,
2. The intermediate classes (i.e., with theoretical water content ranging from about 40% to about 80%) are in fact too diverse since they host cases ranging from “most of the water area is at nadir” to “most of the water area is at far end” of the footprint.
3. The water masks used here are very old (2003) and probably not exhaustive enough regarding the smaller water surfaces [SWBD, 2003]. The low WFR classes from these water masks may have changed.
4. The results may be specific to this part of the Amazon basin or to the season.

The preliminary findings listed below need to be further investigated :

- The backscattered energy and its symmetry in classes with a high WFR is better defined and consistent than those with low WFR.
- Footprints with a very small water content tend have a small RIP Standard Deviation. This would be in agreement with the fact that small bright targets are more specular in general (less sensitive to wind stress) and the small river legs of the downstream Amazon basin do not experience high surface currents ; they are smooth surfaces in most cases. Nevertheless the low WFR class is quite heterogeneous.
- On the opposite footprints which are all over water do have a larger RIP Standard deviation because the footprint exhibit strong backscatter properties in all directions (in all looks).

6. ONGOING WORK AND PERSPECTIVES

We are currently working on two major improvements of the new framework . The first one is to introduce the Pulse-Doppler limited footprint so as to discriminate whether the water pixels are at nadir or not (we introduce the WFRN : Fraction of Water Pixels at NADIR). We also are working on the weighting of the water pixels according to their distance to nadir. We definitely need to process more data and manage to compare WFR classes with equal population in order to refine our investigations.

7. BIBLIOGRAPHY

Bercher N., Calmant S. Fleury S., Dinardo S., Boy F., Picot N. et Benveniste, J. (2014a). “CryoSat-2 over rivers: a present mission, an insight into the future of altimetry”. In Proceedings of the OST/ST, 27-31 October, Lake Constance, Germany. Oral communication.

Fabry, P. and Bercher, N. (2015a). “A step Toward the Automated Production of Water Masks from Sentinel-1 images”, Mapping Water Body from Space Conference, 18-19 March 2015. ESRIN, Frascati. Oral communication.

ESA-UCL, CryoSat-2 Product Handbook, April 2013.

SRTM Water Body Data Product Specific Guidance (v.2.0, March 12, 2003), http://dds.cr.usgs.gov/srtm/version2_1/SWBD/SWBD_Documentation/, NASA/NGA.